Table 1. Effect of antibodies and an inhibitor of cutinase on infection of pea epicotyl by *F. solani pisi*. The inoculum (5 μl) contained 1.2×10^6 spores and the indicated levels of immunoglobulin (IgG) per milliliter. Infection is expressed as the percentage of epicotyl segments infected.

Treatment	Amount	Infection (%)
None		86
Rabbit IgG from serum	4 mg/ml	90
Rabbit IgG from serum	8 mg/ml	87
Rabbit IgG from serum	6 mg/ml	93
IgG from antiserum	1.75 mg/ml	20
IgG from antiserum	3.5 mg/ml	0
Diisopropylfluorophosphate	0.01 m*M*	0
Diisopropylfluorophosphate	1.0 m*M*	0

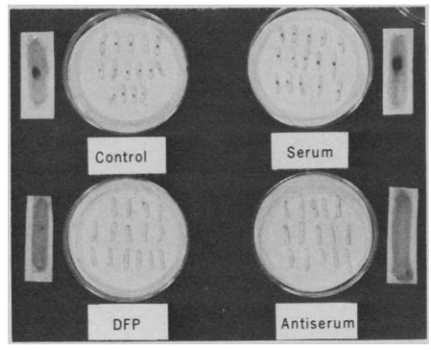

Fig. 1. Photograph of pea epicotyl segments 72 hours after inoculation with 5 μl of conidial suspension of *F. solani pisi* in water (*Control*), water containing 16 mg of protein per milliliter of immunoglobulin fraction from rabbit serum (*Serum*), water containing 1.75 mg of protein per milliliter of rabbit immunoglobulin from antiserum prepared against cutinase (*Antiserum*), and water containing 10 μ*M* DFP. In each case a magnification of a representative tissue segment is also shown.

the dark spot (Fig. 1), were counted; infection is expressed as the percentage of epicotyl segments infected.

Diisopropylfluorophosphate, which is a potent inhibitor of cutinase (*4*), virtually prevented infection of pea epicotyl by *F. solani pisi* (Table 1 and Fig. 1). That the lack of infection was not due to a general toxicity of this chemical to the organism was indicated by microscopic examination of the inoculated region, which showed profuse growth of germinated conidia on the tissue surface, at all of the concentrations of the inhibitor used in this experiment.

Antibody prepared against cutinase prevented infection of the tissue by *F. solani pisi*, whereas the immunoglobulin fraction from rabbits, not immunized with cutinase, had no effect on infection (Fig. 1 and Table 1). Microscopic examination of the inoculated area showed profuse growth of germinated conidia, indicating that immunoglobulin did not adversely affect the germination or growth of the organism. These results clearly show that the specific inhibition of cutinase, known to be caused by the antibodies (*5*), prevented fungal entry into the plant, and thus prevented infection.

Chemical examination of the cuticular polymer of the epicotyl segments by the combined gas-liquid chromatography-mass spectrometry techniques described (*6*) showed that the cutin was composed of chiefly dihydroxypalmitate, ω-hydroxypalmitate, and palmitic acid. These results confirm the previous electron microscopic evidence concerning the presence of cutin on this tissue. The previous finding that *F. solani pisi* excretes cutinase during penetration of its host (*3*) and our finding that specifically blocking the action of this enzyme prevents infection constitute convincing evidence that cutinase is involved in the entry of this pathogen into its host. As was pointed out before (*2*), the tendency to ignore the cuticle, and particularly cutin, as a barrier to pathogen penetration is not justified on the grounds that many pathogens enter the plant via natural openings, because the pathogen must penetrate a cutin layer even when they enter through such channels. Thus, our findings are likely to have widespread application to the understanding of fungal pathogenesis of plants. Even though cuticular penetration is not likely to be involved in the specificity of host selection by fungal pathogens, prevention of penetration would prevent pathogenesis. Since cutinase is not involved in the normal metabolism of either plants or animals, it might be feasible to devise chemicals that are specifically targeted against this enzyme and do not interfere with the metabolism of the host plant or animals which consume the plant products. Thus the present results could be the foundation for the development of enzyme-targeted fungicides ("antipenetrants").

I. B. Maiti
P. E. Kolattukudy
Department of Agricultural Chemistry and Program in Biochemistry and Biophysics, Washington State University, Pullman 99164

References and Notes

1. J. T. Martin, *Annu. Rev. Phytopathol.* **2**, 81 (1964).
2. G. van den Ende and H. F. Linskens, *ibid.* **12**, 247 (1974).
3. M. Shaykh, C. Soliday, P. E. Kolattukudy, *Plant Physiol.* **60**, 170 (1977).
4. R. E. Purdy and P. E. Kolattukudy, *Biochemistry* **14**, 2824 (1975).
5. C. L. Soliday and P. E. Kolattukudy, *Arch. Biochem. Biophys.* **176**, 334 (1976).
6. P. E. Kolattukudy, *Recent Adv. Phytochem.* **11**, 185 (1977).
7. Scientific paper No. 5282, College of Agriculture Research Center, Washington State University, Pullman. Supported in part by NSF grant PCM77-00927 and a grant from the Washington State Tree Fruit Commission. We thank Dr. C. L. Soliday for assistance.

26 January 1979; revised 27 April 1979

A Relationship Between DNA Helix Stability and Recognition Sites for RNA Polymerase

Abstract. *The RNA polymerase binding sites on the DNA of (i) the* aroE-trkA-spc *segment of the* Escherichia coli *genome, (ii) transposon Tn3, (iii) plasmid ColE1, and (iv) coliphage* λ *were mapped by electron microscopy, with the use of the BAC technique; these maps were compared with the maps of the early-melting regions for the same genomes. The results indicate that in all these cases the binding sites for the* E. coli *RNA polymerase lie preferentially in the early melting regions of DNA. These data indicate that helix stability may be an important feature of the multipartite nature of the promoter structure.*

Although the nucleotide sequences of many different promoters and promoter-flanking DNA regions are now available (*1-7*), the analysis of these sequences does not fulfill the original hope of leading to a detailed understanding of the interaction between RNA polymerase and DNA (*1*). There are indications of a relationship between the helix stability along the DNA molecule and the location of those DNA regions that preferentially bind RNA polymerase. For example, we found for the genome of coliphage λ a remarkable correlation between the DNA regions which preferentially melt (*8*) and sites specifically binding *Escherichia coli* RNA polymerase (*9*), as detected by direct visualization by the BAC (benzyldimethyl-C_{12}-C_{14} ammonium chloride) technique (*10*). Our findings are in agreement with analogous results obtained for phage λ by indirect techniques (*11, 12*). To determine whether this correlation holds more generally, we mapped by

electron microscopy the RNA polymerase binding sites and the early melting regions on the following three genomes, which provide natural templates for *E. coli* polymerase: the plasmid ColE1, the transposon Tn*3*, and a portion of the *E. coli* chromosome (*aroE-trkA-spc* segment). The electron microscopic approach was chosen, since this technique is the only one for mapping directly both the RNA polymerase binding sites and the regions of preferential strand separation under partially denaturing conditions [see (*9*)]. We report here that *E. coli* RNA polymerase binding sites lie preferentially in early melting regions of DNA, a result that indicates the multipartite structure of promoters.

The physical orientation of a particular DNA molecule versus its genetic map can be unambiguously determined if the ends are marked by attaching fragments of a well-characterized DNA. We selected λ DNA fragments because the positions of the early melting regions (*8*), the RNA polymerase-binding sites (*9*), and many restriction endonuclease cleavage sites are well known. To map the bacterial *aroE-trkA-spc* segment, we used the intact right arm of the transducing phage λ*spc*2 (*13*) as a reference DNA (Fig. 1a). To map ColE1 and Tn*3*, we constructed a hybrid plasmid consisting of the ColE1::Tn*3* plasmid RSF2124 (*14*) and the *Eco*RI fragments A + F of λ, bearing the cohesive ends of λ in the form of the *cos* site (Fig. 2a) (*15*). These terminal *Eco*RI fragments, which are dissimilar with respect to partial denaturation (*8*) and RNA polymerase binding (*9*), permit orientation of the recombinant plasmid, whereas the cohesive ends served as reference points for measuring. These ends are generated in vivo when plasmids containing λ *cos* site are packaged into λ capsids provided by a helper phage (*17*).

The RNA polymerase binding regions were identified with high specificity by means of electron microscopy and a glutaraldehyde-BAC technique (*9*). As is shown in Figs. 1a and 2a, *E. coli* RNA polymerase molecules bind to defined DNA regions of both genomes represented by the peaks of different heights. On the ColE1::Tn*3*-*cos*λ genome (Fig. 2a), the *Eco*RI-A fragment of λ lacking promoter and polymerase (*9*) can be easily distinguished from the *Eco*RI-F fragment, which carries two strong polymerase binding sites (*9*). Similarly, for the *spc*2 genome the characteristic polymerase binding pattern identified the right arm of this transducing λ phage (*9*) (Fig. 1a), and there is a correspondence between the positions of all known pro-

Table 1. The A + T content of promoter regions (promoter and promoter-flanking sequences) recognized by *E. coli* RNA polymerase, and of the entire genomes.

Origin of sequence bearing promoter region	References	A + T content in percent		
		Promoter*	Promoter and flanking sequence†	Genome‡
φX174A	(*1*)	53.3	60.0	55.2
φX174D	(*1*)	60.0	62.2	55.2
fd*Hpa*D	(*1*)	64.4	63.3	59.2
fd*Hpa*H	(*1, 2*)	77.7	73.3	59.2
SV40	(*1, 3*)	73.3	72.2	59.4
λp_R	(*1, 4*)	55.6	56.7	50 (53)
λp_L	(*1*)	51.1	51.1	50 (53)
λp_{rm}	(*1*)	62.2	63.3	50 (53)
λp_o	(*1, 4*)	66.6	57.8	50 (53)
λp_{c17}	(*1*)	80.0	72.2	50 (53)
P_{gal} (*E. coli*)	(*1*)	64.4	65.5	49
P_{lacZ} (*E. coli*)	(*1*)	55.6	54.4	49
P_{lacI} (*E. coli*)	(*5*)	44.4	45.3	49
P^{Tyr}_{tRNA} (*E. coli*)	(*1*)	46.4	48.8	49
P_{spc} (*E. coli*)	(*6*)	53.3	55.6	49
P_{str} (*E. coli*)	(*6*)	53.3	53.3	49
P_{araBAD} (*E. coli*)	(*7*)	53.3	60.0	49
P_{trp} (*E. coli*)	(*1*)	64.4	62.9	49
P_{trp} (*Salmonella typhimurium*)	(*1*)	64.4	62.4	48
Statistical A + T content		60.2	60.0	51.5

*DNA segment extending from −40 to +5 from the RNA startpoint, defined as +1. †DNA segment extending from −65 to +25 from the RNA startpoint, defined as +1, with the following exceptions: P_{lacI}, −50 to +25; $P_{tyr-tRNA}$, −59 to +25; P_{trp} (*E. coli*), −65 to +24; P_{trp} (*S. typhimurium*), −65 to +20. ‡The data for φX174, fd, and SV40 are based on the sequences of the entire genomes (*1-3*). The numbers in parentheses refer to the 5000 base pairs immunity region of λ (*28*). Other data for λ, *E. coli*, and *S. typhimurium* DNA's are based on (*28*) and (*34*).

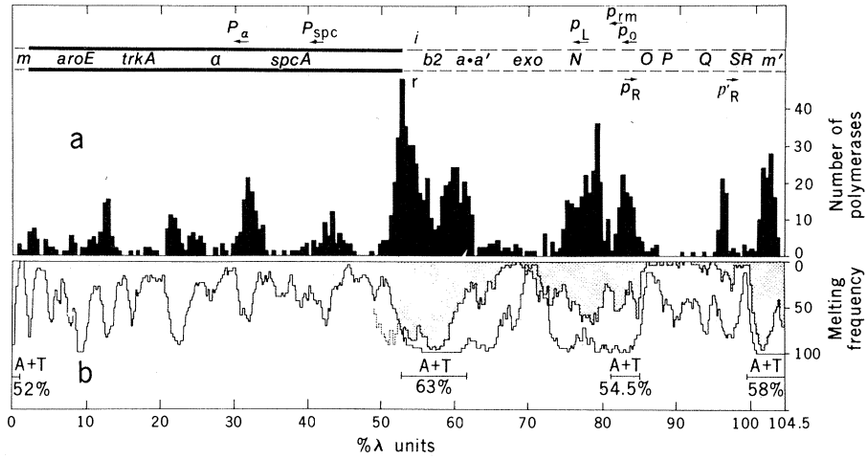

Fig. 1. Comparison of the *E. coli* RNA polymerase binding map (a) of the transducing phage λ*spc*2 with the partial denaturation map (b). Map (a) represents the *aroE-trkA-spc* segment (*13, 26*) of *E. coli* (solid heavy lines) and portions of bacteriophage λ (*27*) (dashed lines). The approximate positions and orientations of the known promoters are indicated by the letter *p* or *P* and a horizontal arrow (*26, 27*). The A + T contents for representative λ fragments (*28*) is specified in map (b) [54.5 percent is determined by sequence; (*4*)]. The positions of the binding sites and early melting regions were mapped in %λ units [a 1-%λ unit corresponds to 480 base pairs, assuming that the λ genome is 48,000 base pairs; see (*9*)]. The RNA polymerase binding sites were identified by the BAC technique (*10*), which permits mapping by electron microscopy of specifically bound protein molecules on double- and single-stranded nucleic acids (*9, 29*). The procedure described (*9*) was followed, except that (i) the initial molar ratio of polymerase to DNA was 40:1, (ii) the dehydration was performed in 90 percent methanol, and (iii) when the relative humidity in the laboratory was lower than 50 percent, the carbon films were floated for 10 minutes on an aqueous solution containing ethidium bromide (30 μg/ml), washed for another 10 minutes by floating on twice-distilled water, and blotted dry on filter paper just before use (*30*). In histogram (a), the positions of a total of 1130 bound RNA polymerases were measured on 112 DNA molecules. Polymerases bound to the DNA termini were not recorded. For the open histogram in map (b), 25 DNA molecules prepared by alkali denaturation [see (*8*)] at *p*H 11.3, for 60 minutes were analyzed. The superimposed alkali-denaturation map was obtained under milder conditions by R. B. Inman [cross-hatched areas correspond to the λ portion of λ*spc*2 (47.7 to 100 %λ on the λ map and 52.2 to 104.5 %λ on λ*spc*2 map above) and the dotted line corresponds to λ DNA, which is substituted by *E. coli* DNA in λ*spc*2 (44.5 to 47.7 %λ on the λ map)].

0036-8075/79/0803-0509$00.50/0

moters and the peaks indicating polymerase binding regions (Figs. 1a and 2a).

After partial denaturation of the above genomes by alkali (*8*), we mapped the sites of strand separation along the DNA molecules (Figs. 1b and 2b), which correspond to A · T-rich regions (adenine, thymine). The distinct peaks representing less stable DNA regions are not necessarily indicative of a very high local concentration of A and T bases, since it has been shown that only a few percent increase in the A + T content if extended over a few hundreds of base pairs gives rise to a distinct sharp peak in a denaturation map (*18*). The maps of the polymerase binding regions were carefully aligned with the denaturation maps in Figs. 1 and 2, although a perfect alignment is difficult because of the differences in length between single- and double-stranded DNA under denaturing conditions. Any misalignment, however, has to be minimal, because the peaks to the left of 70 %λ (percent lambda units) in Fig. 2b must be on the ColE1::Tn*3* DNA, since they were not observed for λ molecules and since the leftmost peak, at about 45 %λ in Fig. 2b, was observed on a mini ColE1 derivative (*16*). Moreover, the frequency of melting displayed by the λ*spc*2 genome, when compared with λ^+, diminishes to the left of 52.2 %λ (Fig. 1b), which is in perfect agreement with heteroduplex mapping of the boundary between λ and bacterial DNA (*13*), the latter of a higher guanine plus cytosine (G + C) content.

Comparing the polymerase binding and the partial denaturation maps (Figs. 1 and 2) permits us to conclude that polymerase binding sites lie preferentially within early melting regions. This correlation, however, is not quantitatively perfect.

To extend this correlation to the sequenced promoter regions, we analyzed the A + T content of 19 published sequences (*1*-*7*) recognized by *E. coli* RNA polymerase. Comparing the A + T contents of the promoters or the promoter-flanking regions with those of the entire genomes shows that the A + T contents of most promoters and flanking regions are significantly higher than those of the corresponding genomes (Table 1). This agrees with the notion that promoters are preferentially located in early melting regions. Moreover, this also seems to hold for templates not naturally utilized by *E. coli* RNA polymerase (Table 1) (*19*). Two exceptions are promoters for the $tRNA^{Tyr}$ (tyrosine transfer RNA) and the *lac*I genes, but there are no denaturation maps available to determine whether adjoining regions might be AT-rich. Also the p_L promoter, although containing more than 50 percent A + T, is less AT-rich than the corresponding DNA segment of about 10 percent of the length of λ.

Using a single-strand specific nuclease as a probe for the dynamic structure of DNA (*20*), Chan *et al.* (*21*) have shown that restriction fragments originating from early melting regions of the λ genome were particularly susceptible to such endonucleases, an indication of a high frequency of transient opening of base pairs (breathing). Therefore, such less stable DNA regions could aid in recognition of a promoter by providing transiently opened DNA stretches and then could further facilitate RNA polymerase-mediated strand separation (*22*). In fact, factors that stabilize helical structures—for example, high ionic strength and low temperature—inhibit polymerase binding (*23*), whereas factors that destabilize base-paired DNA—such as elevated temperature, denaturing agents, and negative supertwists in the template promote polymerase binding (*24*).

However, an early melting region is not sufficient for the formation of a specific and stable polymerase-DNA complex, since such regions do not bind per se RNA polymerases, as is shown in Fig. 1b around the site 90 %λ (*9*, *11*). Thus, promoter sequences may provide the necessary points of contact, permitting specific polymerase binding and selective initiation of transcription. In fact, there appear to be at least two sites of approximate sequence homology (*1*). One site is centered about ten base pairs from the startpoint of transcription and another lies about 25 to 40 base pairs from the startpoint. Deoxyribonuclease protection experiments show that this region is required for the formation of a stable binary complex but probably not for the maintenance of that complex [see (*1*) and (*25*)].

Our data strongly suggest that the helix stability in a promoter region is an important structural element and indicate a multipartite structure of a promoter: several specific contact points for the RNA polymerase are embedded in a more or less AT-rich and thus unstable DNA re-

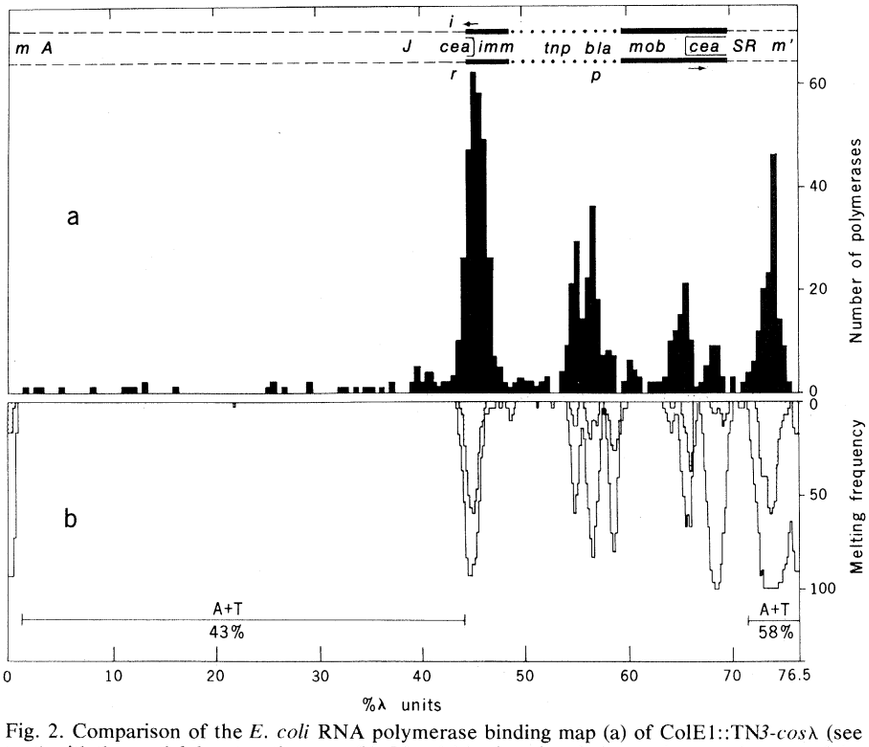

Fig. 2. Comparison of the *E. coli* RNA polymerase binding map (a) of ColE1::TN*3*-*cos*λ (see text) with the partial denaturation map (b). Map (a) is given in relation to the genetic maps of the transposon Tn*3* (dotted lines) (*31*), the plasmid ColE1 (solid heavy lines) (*32*), and portions of bacteriophage λ (dashed lines) (*27*). Symbol *p* represents the most likely position of the promoter for the β-lactamase (*bla*) gene on the Tn*3* transposon (*15*). Symbol *tnp* indicates transposition-related genes on Tn*3* (*31*). The arrows indicate the orientation and possible sites of the initiation of transcription on the ColE1 plasmid (*32*, *33*). ColE1 termini were created by *Eco*RI which cleaves the colicin (*cea*) determinant (shown by cut box). In the histogram (a) 113 DNA molecules bearing 783 RNA polymerases (exclusive of polymerases bound to termini) were analyzed. The initial molar ratio of RNA polymerase to DNA was 15:1. In map (b), the cross-hatched histogram represents 19 molecules denatured at *p*H 11.3 for 15 minutes, and the open histogram represents 30 molecules denatured at the same *p*H for 60 minutes. The remaining experimental details and source of the A + T data are as outlined in Fig. 1.

gion, which facilitates the formation of the open complex. Consequently, the recognition of a specific binding site and the formation of a stable (open) polymerase-DNA complex ready for initiation depends on the quality of the contact points and on the stability of the helix, thus providing a simple explanation why the correlation between frequencies of polymerase binding and localized DNA melting is not perfect (see Figs. 1 and 2). Therefore, the helix stability in a promoter and its flanking DNA regions may play an important role in setting the level of transcription and consequently may have a regulatory function in gene expression. In this regard, it may be significant that the nucleotide sequence with the lowest A + T content in Table 1 codes for an unusually weak promoter, namely P_{lacI} (*5*).

H. J. VOLLENWEIDER*
M. FIANDT, W. SZYBALSKI
McArdle Laboratory for Cancer Research, University of Wisconsin, Madison 53706

References and Notes

1. These sequences are compiled or citations are provided by G. E. G. Scherer, M. D. Walkinshaw, and S. Arnott [*Nucleic Acids Res.* **5**, 3759 (1978)].
2. H. Schaller, personal communication.
3. V. B. Reddy, B. Thimmappaya, R. Dhar, K. N. Subramanian, B. S. Zain, J. Pan, P. K. Ghosh, M. L. Celma, S. M. Weissman, *Science* **200**, 494 (1978).
4. E. Schwarz, G. Scherer, G. Hobom, H. Kössel, *Nature (London)* **272**, 410 (1978).
5. M. P. Calos, *ibid.* **274**, 762 (1978).
6. L. E. Post, E. E. Arfsten, F. Reusser, M. Nomura, *Cell* **15**, 215 (1978).
7. L. Greenfield, T. Boone, G. Wilcox, *Proc. Natl. Acad. Sci. U.S.A.* **75**, 4724 (1978).
8. R. B. Inman and M. Schnös, *J. Mol. Biol.* **49**, 93 (1970).
9. H. J. Vollenweider and W. Szybalski, *ibid.* **123**, 485 (1978).
10. H. J. Vollenweider, J. M. Sogo, T. Koller, *Proc. Natl. Acad. Sci. U.S.A.* **72**, 83 (1975); H. J. Vollenweider, T. Koller, J. Parello, J. M. Sogo, *ibid.* **73**, 4125 (1976); H. J. Vollenweider, A. James, W. Szybalski, *ibid.* **75**, 710 (1978).
11. B. B. Jones *et al.*, *ibid.* **74**, 4914 (1977).
12. P. Botchan, *J. Mol. Biol.* **105**, 161 (1976).
13. M. Fiandt, W. Szybalski, F. R. Blattner, S. R. Jaskunas, L. Lindahl, M. Nomura, *ibid.* **106**, 817 (1976).
14. M. So, R. Gill, S. Falkow, *Mol. Gen. Genet.* **142**, 239 (1975).
15. H. J. Vollenweider, M. Fiandt, W. Szybalski, *J. Mol. Biol.*, in press.
16. R. K. Patient, S. C. Hardies, J. E. Larson, R. B. Inman, L. E. Maquat, R. D. Wells, *J. Biol. Chem.* **254**, 5548 (1979).
17. H. J. Vollenweider, M. Fiandt, E. C. Rosenvold, W. Szybalski, *J. Mol. Biol.*, in press.
18. G. I. Karataev, V. I. Permogorov, A. V. Vologodskii, M. D. Frank-Kamenetskii, *Nucleic Acids Res.* **5**, 2493 (1978).
19. B. Lescure, P. Oudet, P. Chambon, M. Yaniv, *J. Mol. Biol.* **108**, 83 (1976).
20. L. Wingert and P. H. von Hippel, *Biochim. Biophys. Acta* **157**, 114 (1968).
21. H. W. Chan, J. B. Dodgson, R. D. Wells, *Biochemistry* **16**, 2356 (1977).
22. M. J. Chamberlin, in *RNA Polymerase*, R. Losick and M. J. Chamberlin, Eds. (Cold Spring Harbor Laboratory, Cold Spring Harbor, N.Y., 1976), pp. 155–191.
23. W. Mangel and M. J. Chamberlin, *J. Biol. Chem.* **249**, 3002 (1974); S. Nakanishi, S. Adhya, M. Gottesman, I. Pastan, *ibid.* **250**, 8202 (1975); W. Mangel and M. J. Chamberlin, *ibid.* **249**, 3007 (1974); W. Zillig, K. Zechel, D. Rabussay, M. Schaehner, V. Sethi, P. Palm, A. Heil, W. Seifert, *Cold Spring Harbor Symp. Quant. Biol.* **35**, 47 (1970).
24. S. Nakanishi, S. Adhya, M. Gottesman, I. Pastan, *J. Biol. Chem.* **249**, 4050 (1974); A. Travers, *Eur. J. Biochem.* **47**, 435 (1974); M. Crepin, R. Cukier-Kahn, F. Gros, *Proc. Natl. Acad. Sci. U.S.A.* **72**, 333 (1975); P. Botchan, J. Wang, H. Echols, *ibid.* **70**, 3077 (1973); Y. Hayashi and M. Hayashi, *Biochemistry* **10**, 4212 (1971); J. Richardson, *J. Mol. Biol.* **91**, 477 (1975); J. Wang, *ibid.* **87**, 797 (1974).
25. W. Gilbert, in *RNA Polymerase*, R. Losick and M. J. Chamberlin, Eds. (Cold Spring Harbor Laboratory, Cold Spring Harbor, N.Y., 1976), pp. 193–205.
26. S. R. Jaskunas, A. M. Fallon, M. Nomura, *J. Biol. Chem.* **252**, 7323 (1977).
27. E. H. Szybalski and W. Szybalski, *Gene*, in press.
28. N. Davidson and W. Szybalski, in *The Bacteriophage Lambda*, A. D. Hershey, Ed. (Cold Spring Harbor Laboratory, Cold Spring Harbor, N.Y., 1971), pp. 45–82.
29. H. J. Vollenweider, T. Koller, H. Weber, C. Weissmann, *J. Mol. Biol.* **101**, 367 (1976).
30. T. Koller and H. J. Vollenweider, unpublished results.
31. F. Heffron, M. So, B. J. McCarthy, *Proc. Natl. Acad. Sci. U.S.A.* **75**, 6012 (1978).
32. G. Dougan, M. Saul, G. Warren, D. Sheratt, *Mol. Gen. Genet.* **158**, 325 (1978).
33. R. K. Patient, personal communication.
34. W. M. Normore, in *Handbook of Biochemistry and Molecular Biology, Nucleic Acids*, G. C. Fasman, Ed. (CRC Press, Cleveland, 1976), vol. 2, pp. 110 and 113.
35. Dr. R. B. Inman generously supplied us with a denaturation map of λ DNA (Fig. 1b), Dr. R. R. Burgess with *E. coli* RNA polymerase, and Drs. L. E. Post and M. Nomura with λ*spc*2 phage. We thank Drs. R. R. Burgess, R. K. Patient, and W. Reznikoff for critically reading the manuscript and Dr. E. Szybalski for editorial help. We thank L. Wilson and P. Speth for preparing large quantities of phage. This work was supported by the NIH program project grant CA-07175 and training grant No. T32-CA-09075.
* Present address: MRC Laboratory of Molecular Biology, Hills Road, Cambridge CB22QH, England.

1 January 1979; revised 26 April 1979

Orientation Anisotropy of Visual Stimuli in Rhesus Monkey: A Behavioral Study

Abstract. *The contrast sensitivity of the rhesus monkey was tested, according to a modified reaction-time paradigm, for sine-wave grating targets at different orientations. The monkey possesses an oblique effect slightly larger than that of humans. A reaction time analysis showed the oblique effect to be a suprathreshold as well as a threshold phenomenon. The presence of this effect further strengthens the use of the monkey as a model for the human visual system.*

The human ability to resolve grating patterns with a vertical or horizontal orientation better than those with an oblique orientation has been well documented (*1*). We know that this orientation anisotropy or oblique effect is of neural origin, because it is present even if the optics of the eye are bypassed and laser interference fringes are formed directly on the retina (*2*). The oblique effect, present only for central vision, has many of the characteristics of meridional amblyopia, which is considered to be due to environmental factors during early development (*3*). Attempts to obtain supporting evidence for these environmental influences are contradictory since some investigators (*4*) have found evidence for an oblique effect in infants and others (*5*) have not, although recent evidence indicates that this discrepancy may be due to differences in measurement techniques (*6*). Attempts to determine the neural mechanism for an orientation anisotropy have also been contradictory (*7–9*). Mansfield has reported that in monkeys a preponderance of neurons in the striate cortex with receptive fields in the fovea respond optimally to vertical or horizontal stimuli. Additonally, visual evoked responses from the monkey indicate the presence of an oblique effect. However, Finlay *et al.* and Poggio *et al.* (*9*) have reported that there is not a significant orientation bias for monkey foveal striate neurons. There are, of course, several possible reasons for the discrepancy.

The first question to be answered before investigations into the neural mechanisms of the oblique effect become significant is: Does the monkey behaviorally demonstrate an oblique effect? We now present a behavioral demonstration of the oblique effect in two rhesus monkeys. We also show how the oblique effect varies as a function of the spatial frequency of the stimulus and provide behavioral data indicating that the oblique effect is a suprathreshold as well as a threshold phenomenon (*10*).

Monkeys were trained to detect sinusoidal grating patterns generated on a cathode-ray tube (CRT) according to the method described by Campbell and Green (*11*). The CRT was masked to subtend a 4° visual angle at 114 cm (the viewing distance). The mean luminance of the visual display, 67 cd/m^2, remained constant for all contrast levels and spatial frequencies. The oscilloscope was cradled in an apparatus that could be rotated about the center of the display in 10° increments from 0° through 170° with additional stops at 45° and 135°.

The behavioral procedures used for the data collection were a modification of the reaction time procedure used previously in increment threshold experiments (*12*). The monkeys were trained to press and hold a lever at the start of each trial, which was signaled by the onset of

0036-8075/79/0803-0511$00.50/0